(54) (a) B. E. Mann, *J. Chem. Soc., Dalton Trans.*, 2012 (1973); (b) G. M. Bodner and L. J. Todd, *Inorg. Chem.*, **13**, 360 (1974).
(55) (a) J. A. Pople, *Mol. Phys.*, 7, 310 (1964). A more complete discussion of ^{13}C shifts in metal carbonyls has been presented.[30,46,54,55b,c] (b) H. Mahnke, R. J. Clark, R. Rosanske, and R. K. Shelline, *J. Chem. Phys.*, **60**, 2997 (1974). (c) P. S. Braterman, D. W. Milne, E. W. Randall, and E. Rosenberg, *J. Chem. Soc., Dalton Trans.*, 1027 (1973).
(56) Various other mechanistic pathways produce chemically less reasonable intermediates that have less favorable valence electron distribution, as has been discussed elsewhere.[23-26,51]
(57) R. D. Adams, D. M. Collins, and F. A. Cotton, *J. Am. Chem. Soc.*, **96**, 749 (1974); *Inorg. Chem.*, **13**, 1086 (1974).
(58) P. McArdle and A. R. Manning, *J. Chem. Soc. A*, 717 (1971).
(59) This type mechanism has been invoked for ^{13}CO interchange in some rhodium carbonyls: J. Evans, B. F. G. Johnson, J. Lewis, and T. W. Matheson, *J. Chem. Soc., Chem. Commun.*, 576 (1975).

A Crystal Field Model for Calculating Mössbauer Quadrupole Splittings of Iron Complexes. Application to Pseudo-D_3 and Pseudo-D_{2h} Low-Spin Ferrous Complexes

Susan C. Jackels,* Ernest R. Davidson, and Norman J. Rose

Contribution from the Chemistry Department, University of Washington, Seattle, Washington 98195. *Received August 21, 1975*

Abstract: In this paper we present a crystal field method for calculating an approximate Mössbauer quadrupole splitting specially designed for iron complexes with low symmetry. The main features of the method are (1) evaluation of the entire efg tensor from the point charges and the 3d crystal field orbital populations, and (2) diagonalization of the efg tensor to obtain the principal tensor elements. Application of the method to two classes of low-spin ferrous compounds having either pseudo-D_3 or pseudo-D_{2h} symmetry indicates that the crystal field approach correctly predicts the sign of the quadrupole splitting for these complexes. Calculations performed on model coordination polyhedra for the two classes of complexes show which geometrical and/or charge parameters are important in determining the sign of the quadrupole splitting.

I. Introduction

The availability of Mössbauer spectra for a rather wide variety of iron complexes has stimulated the development of models which are intended to account for and effectively predict the relationship between (1) the magnitude and sign of the quadrupole splitting (qs) obtained from the spectra and (2) the nature of the structure and bonding exhibited by the complexes. The qs arises from the interaction of the quadrupole moment of the ^{57}Fe nucleus in its excited state ($I = 3/2$) with the asymmetric electronic charge distribution surrounding the iron nucleus. Having the ability to interpret the qs data, therefore, can lead directly to some understanding of the changes in the electron distribution at the iron atom which are caused by substituting one kind of ligating atom for another (i.e., oxygen for nitrogen) and/or changing the geometrical arrangement of the ligating atoms.

Various approaches have been employed to predict the sign and magnitude of the qs for iron complexes.[1-6] The central element in each of these approaches is the manner in which the electric field gradient (efg) at the iron nucleus is estimated. The methods for approximating the efg at the iron nucleus span the range from semiempirical models using partial field gradients[1] to highly theoretical models[2] including the consideration of Coulomb repulsion of 3d electrons in the point symmetry of the complex and spin-orbit interactions. Between these extremes various models have been put forth utilizing the features that (1) the major contribution to the efg at the iron nucleus stems from the partially filled 3d shell[3-5] and other valence electrons are either neglected[1] or included[6] when suitable MO calculations are available, (2) the efg arising from the polarization of core electrons by the asymmetric, partially filled valence shell is either neglected[6] or approximated by use of the Sternheimer coefficients,[1,7] and (3) the chosen coordinate system is the principal one,[1] i.e., diagonalization of the efg tensor is "automatically" done by selection of the coordinate system in order to calculate the quadrupole coupling parameters. The latter assumption greatly simplifies the calculation in that only the diagonal elements of the efg tensor need be evaluated. Unfortunately for low symmetry complexes the a priori assignment of the orientation of the principal axes is difficult if not impossible.

Our goal in this paper is to generalize the well-known methods for calculating the efg from valence orbital and point charge contributions and to test the application to low symmetry complexes. The principal feature of the model being presented here is that the major source of the efg is assumed to be the asymmetric d electron distribution arising from the incomplete population of the d shell combined with the mixing of the d orbitals by the interaction of the crystal field. Strong support for this feature comes from the recent calculation of Goddard and Olafson[8] for the hemoglobin case in which it was shown that the populated d orbitals alone can account for the observed large quadrupole splitting. This concept is in direct contrast to the partial field gradient method which assumes that the source of the field gradient is covalency effects in which ligands donate electrons into the unoccupied hybridized orbitals.[9] The experimentally observed quadrupole splittings are undoubtedly caused by a combination of both effects; however, it has not been generally appreciated that the occupied d orbitals alone may be responsible for the greatest share in determining the qs for complexes such as those of low-spin iron(II) with ligands capable of substantial covalent interaction.[1a] The model being presented here is also distinguished from other similar treatments in that the *entire* efg tensor is first evaluated from the occupied 3d crystal field orbitals and point charges and is then diagonalized to obtain the principal elements.

The method is applied to two classes of low-spin iron(II) complexes, one characterized by pseudo-D_3 symmetry and the other by pseudo-D_{2h} symmetry. A series of calculations on model coordination polyhedra is presented to illustrate which

Table I. Efg Tensor Operators

$$\nu_{xx} = er^{-3}(3\sin^2\theta\cos^2\phi - 1)$$
$$\nu_{yy} = er^{-3}(3\sin^2\theta\sin^2\phi - 1)$$
$$\nu_{zz} = er^{-3}(3\cos^2\theta - 1)$$
$$\nu_{xy} = \nu_{yx} = er^{-3}(3\sin^2\theta\sin\phi\cos\phi)$$
$$\nu_{yz} = \nu_{zy} = er^{-3}(3\sin\theta\cos\theta\sin\phi)$$

molecular parameters are important in determining the sign and magnitude of the qs for the two classes of complexes studied.

II. Theoretical Model

The Mössbauer quadrupole splitting is calculated from the efg tensor[1,10] evaluated at the iron nucleus by using eq 1

$$\text{qs} = \frac{1}{2}e^2Qq(1 + \eta^2/3)^{1/2} \qquad (1)$$

where e is the charge on an electron and Q is the quadrupole moment of the ^{57}Fe nucleus. The quantities q and η are related to the diagonal efg tensor elements by eq $= V_{zz}$ and $\eta = (V_{xx} - V_{yy})/V_{zz}$, where the axes are chosen such that $|V_{zz}| \geq |V_{yy}| \geq |V_{xx}|$ and $V_{xy} = V_{xz} = V_{yz} = 0$. This coordinate system which diagonalizes the efg tensor is referred to as the principal coordinate system.

In order to calculate the qs, the efg tensor is evaluated at the iron nucleus. In the model being presented here, the efg tensor elements, V_{pq}, are expressed as a sum of point charge and crystal field orbital population contributions (eq 2).

$$V_{pq} = (1 - \gamma_\infty)V_{pq}(\text{point charge}) + (1 - R)V_{pq}(\text{crystal field}) \qquad (2)$$

These two contributions are combined using the Sternheimer factors,[7] $1 - \gamma_\infty$ and $1 - R$, which approximate the efg from polarization of inner core electrons due to the point charges and d electron distribution. Unfortunately, no values of R and γ_∞ are available which are applicable to the cases being considered here (i.e., iron(II) bound in an asymmetric strong ligand field environment). Eicher and Trautwein[11] have used a value of zero for R in iron porphyrin complexes. In general R is a small positive number in the range 0 to +0.2.[12] In the absence of any more relevant evaluations of R we have used Freeman and Watson's value[13] of 0.32 as calculated for high spin ferrous ion to include the polarization of the ferric like core (^{6}S, 3d^5) due to the sixth d electron. It will be seen below that the chosen R value strongly affects the magnitude of the calculated qs (the point charge contribution is often an order of magnitude smaller than the crystal field orbital contribution, vide infra). We will therefore be most interested in the predicted trends in qs rather than in the magnitudes of the calculated qs. For γ_∞ we have used the ferrous free ion estimate[14] of −11. In eq 2 Vpq(point charge) is the sum of the efg's generated by individual point charges, Z_i, placed at the ligand positions, r_i, θ_i, ϕ_i.

$$V_{pq}(\text{point charge}) = \sum_i Z_i\nu_{pq}(r_i,\theta_i,\phi_i) \qquad (3)$$

where the $\nu_{pq}(r_i,\theta_i,\phi_i)$ are the efg tensor operators[1] (Table I) for calculating the electric field gradient tensor elements at the origin (iron nucleus) due to a point charge at (r,θ,ϕ).

The V_{pq}(crystal field) term in eq 2 consists of the expectation values of the efg tensor operators, ν_{pq} (Table I) summed over the occupied crystal field orbitals:

$$V_{pq}(\text{crystal field}) = \sum_k -n_k\langle\psi_k|\nu_{pq}|\psi_k\rangle \qquad (4)$$

In eq 4, n_k is the number of electrons in the kth orbital and ψ_k is the linear combination of 3d orbitals describing the kth orbital. Each 3d orbital basis function may be approximated as a product of a real spherical polynomial, $Y_2^\lambda(\theta,\phi)$, $\lambda = 1, 2, \ldots, 5$, and a radial function, $R_{3d}(r)$. For the radial function, Clementi's representation of atomic SCF orbitals[15] by a linear combination of five Slater-type radial functions was used. The negative sign in eq 4 is included for the −1 charge on an electron.

Table II. Complete List of Nonzero Angular Integrals (see eq 5) Contributing to the Electronic Efg Tensor

Tensor element	d_1	d_2	$\langle y_2^{d_1}\|A_{pq}(\theta,\phi)\|y_2^{d_2}\rangle$
V_{zz}	z^2	z^2	$+4/7$
	x^2-y^2	x^2-y^2	$-4/7$
	xy	xy	$-4/7$
	yz	yz	$+2/7$
	xz	xz	$+2/7$
V_{xx}	z^2	z^2	$-2/7$
	x^2-y^2	x^2-y^2	$+2/7$
	xy	xy	$+2/7$
	xz	xz	$+2/7$
	yz	yz	$-4/7$
	z^2	x^2-y^2	$-(2/7)\sqrt{3}$
V_{yy}	z^2	z^2	$-2/7$
	x^2-y^2	x^2-y^2	$+2/7$
	xy	xy	$+2/7$
	xz	xz	$-4/7$
	yz	yz	$+2/7$
	z^2	x^2-y^2	$+(2/7)\sqrt{3}$
V_{zx} (= V_{xz})	xy	yz	$+3/7$
	xz	x^2-y^2	$+3/7$
	xz	z^2	$+(1/7)\sqrt{3}$
V_{yx} (= V_{xy})	yz	xz	$+3/7$
	z^2	xy	$-(2/7)\sqrt{3}$
V_{zy} (= V_{yz})	xy	xz	$+3/7$
	x^2-y^2	yz	$-3/7$
	z^2	yz	$-(1/7)\sqrt{3}$

Because both the ψ_k's and the ν_{pq}'s in eq 4 can be written as a product of a purely radial function and a purely angular function, each integral can be expanded, factored, and rewritten as follows

$$\langle\psi_k|\nu_{pq}|\psi_k\rangle = \sum_{\lambda,\lambda'} C_{k\lambda}C_{k\lambda'}\langle R_{3d}(r)|er^{-3}|R_{3d}(r)\rangle \times \langle Y_2^\lambda(\theta,\phi)|A_{pq}(\theta,\phi)|Y_2^{\lambda'}(\theta,\phi)\rangle \qquad (5)$$

where the $C_{k\lambda}$'s are the coefficients of the d orbital basis functions in the crystal field orbital, $\psi_k = R_{3d}(r)\,\Sigma_\lambda C_{k\lambda}Y_2^\lambda$, and $A_{pq}(\theta,\phi)$ is the angular portion of the ν_{pq} operator. The radial integral in eq 5 has been evaluated[16] from Clementi's radial function for Fe(II), [Ar]3d^6 ^{5}D, as 34.3278 (1/Å^3). Its value is rather insensitive to overall charge on the iron atom, decreasing only slightly to 33.5937 (1/Å^3) for iron(0), [Ar] 3d^{6}4s^2 ^{5}D. This insensitivity is understandable in view of the fact that removal of 4s electrons does not appreciably deshield the 3d electrons. The angular integrals in eq 5 can be evaluated for all the possible combinations of the A_{pq} and the Y_2^λ. For example,

$$\langle Y_2^{z^2}|A_{xx}|Y_2^{x^2-y^2}\rangle = \int_{\theta=0}^{2\pi}\int_{\phi=0}^{\pi}(5/16\pi)\sqrt{3} \times (3\cos^2\theta - 1)(3\sin^2\theta\cos^2\phi - 1)(\sin^2\theta\cos 2\phi) \times \sin\theta\,d\theta\,d\phi = -(2/7)\sqrt{3}$$

Of the 90 integrals possible, 65 are zero by symmetry; the remaining 25 have been evaluated and are given in Table II.

Calculation of the qs may be summarized as follows. The point charge and electronic contributions are evaluated by performing the sums in eq 3 and 5 using the ligand positions and charges and using the crystal field orbitals and their

Table III. Observed and Calculated Mössbauer Parameters for Some Pseudo-D_3 Complexes

Complex	Obsd qs[a]	Obsd η[a]	Calcd qs[b]	Calcd η[b]
$[Fe(DMG)_3(BF)_2]$	+1.0	0	+4.4	0.002
$[Fe(PccBF)]^+$	+0.95	0.27	+4.9	0.4
$[Fe(BDH)_3(CH_2)_6]^{2+}$	+0.5	~0	+4.9	0.18
$[Fe(phen)_3]^{2+}$	−0.29	0.39	−4.8	0.16
$[Fe(py_3tren)]^{2+}$	−0.38	0.31	−5.7	0.07
$[Fe(py_3tame)]^{2+}$	−0.41	0.28	−1.6	0.53

[a] The data are taken from ref 20. Measurements made at 77 or 4.2 K (mm/s) relative to sodium nitroprusside. [b] Calculated from crystallographic atom positions; see figure 2 and Table IV.

Table IV

Complex	Average structural parameters[a] r (Å)	θ' (deg)	$\Delta\phi$ (deg)	Ref
$[Fe(DMG)_3(BF)_2]$	1.93	52.7	21	24
$[Fe(PccBF)]^+$	1.934	50.8		
	1.981[b]	53.1[b]	21.7	25
$[Fe(BDH)_3(CH_2)_6]^{2+}$	1.93	52.7	20.8	26[c]
$[Fe(phen)_3]^{2+}$	1.97	57.7	55	27, 28
$[Fe(py_3tren)]^{2+}$	1.94	57.8		
	1.96[b]	59.0[b]	54	29
$[Fe(py_3tame)]^{2+}$	1.910	52.6		
	2.024[b]	56.4[b]	43	30

[a] Mean values calculated from crystallographic atom positions (see reference), r, θ', and $\Delta\phi$ as defined in Figure 2. [b] Pyridine nitrogen atoms. [c] Our shorthand notation for Goedken's clathrochelate.[26]

populations derived from the spin multiplicity of the complex. The sums from eq 3 and 5 are combined in eq 2. In this way each of the nine efg tensor elements is evaluated. Diagonalization of the resulting V matrix is equivalent to rotation of the coordinate system to coincide with the principal coordinate system. The eigenvalues of V are the diagonal elements in the principal coordinate system and they can be used to obtain q and η as explained following eq 1. Finally, using the value of 0.15 barn[17] for Q in eq 1 for an iron nucleus and using the Doppler effect, the qs becomes

$$\text{qs(mm/s)} = 0.2255(1 + \eta^2/3)^{1/2}(q)(1/\text{Å}^3)$$

in practical units.

III. Results and Discussion

A. General Results. In order to test the application of the model presented above, a computer program was written to calculate the qs for any given set of ligating atom positions and charges. Two general arrangements of six point charges were chosen for investigation. These arrangements serve as representations for two groups of low-spin ferrous complexes for which crystallographic and, for one arrangement, extensive Mössbauer data are available. In the following section the general results from all the calculations are presented. Then, the results for each ligand arrangement are described. Finally, calculations on model coordination polyhedra (in which selected stereochemical or ligand charge parameters are varied) show which factors are most important in determining the sign of the qs.

Several general results have been obtained from all the calculations performed to date on the systems to be described below. First, the crystal field orbital term of the efg (eq 2 and 4 above) is always significantly larger (up to a factor of 10 depending upon the magnitude of the point charges selected) than the point charge term, after Sternheimer corrections are applied. This finding is in agreement with the previous results of others.[18] The effect is due primarily to the different magnitudes of the $\langle 1/r^3 \rangle$ factor in these terms. For the d electrons the average distance from the nucleus is small (<1 Å) and therefore $\langle 1/r^3 \rangle$ is much larger than for the point charges. Another general result noted in all calculations is that the point charge efg term is always opposite in sign to the orbital efg term even though both contributions arise from the distribution of negative charge about the iron nucleus (this has also been noted before[19]).

Since, for the low-spin d^6 configuration, the d electrons are "concentrated" in the regions between the ligands, the efg from the orbital electron distribution will be quite different from that generated from the point charges. A third general result follows from the first two. Because the orbital efg term is much larger than the term from the point charges, the orbital term always determines the sign of the efg and likewise the sign of the qs.

B. Complexes with Pseudo-D_3 Symmetry. The first arrangement of six ligands is representative of complexes containing six imine or pyridine nitrogen donor atoms. qs data for some low-spin complexes of this type are given in Table III. The data reveal that among the six complexes there are large variations in both the sign and magnitude of the qs, spanning a range from +1.0 to −0.41 mm/s. Crystallographic donor atom positions (references in Table IV) available for all six complexes were used to calculate the qs for each complex (Table III). For these calculations equal assumed charges of −0.2e were placed at each donor atom position.[21] For three of the complexes in Table III it is explicitly proper to represent all the ligating atoms by the same charge since the six atoms are chemically equivalent. The other three complexes each possess six nitrogen atoms which are in sp^2 hybridization and are part of an N=C—C=N linkage. In general Fe(II) complexes containing three of these α-diimine linkages are low spin, the classical examples being $[Fe(bpy)_3]^{2+}$ and $[Fe(phen)_3]^{2+}$. Since the py_3tame and py_3tren ligands are comparable in position in the spectrochemical series to phen and bpy, the use of only one value of charge to represent all the ligating atoms in the former two ligands seems justified.[22] The case for using only one value of charge to represent the six donor atoms of PccBF is not as strong.[22]

A plot of the calculated results vs. the experimental qs data is shown in Figure 1. The plot shows that in each case the sign of the qs is correctly predicted, and the magnitudes are correlated with the experimental values. However, the magnitudes of the calculated qs are a factor of 4 to 16 greater than the observed qs. The calculated asymmetry parameters (Table III) are not correlated well at all with the experimental values.

In our model there are several factors which could contribute to inflated values of the qs. First, there is the problem of the selection of the magnitude of point charges to use and the distance from the metal ion that they should be placed. Secondly, there are all the classical limitations associated with the use of the crystal field formalism for representing the electron distribution about the metal ion. Thirdly the most important sources of uncertainty are the several "constants", namely, $\langle 1/r^3 \rangle$, the Sternheimer coefficients, and the ^{57}Fe nuclear quadrupole moment, all of which are approximations. The free ion value of $\langle 1/r^3 \rangle$ evaluated from the crystal field Slater orbitals is certainly not the same for an iron atom in a strong ligand field complex and is probably not constant among the complexes. The most difficult problem is that the Sternheimer corrections have been developed for free ion iron(II) with the core including five d electrons.[23] These corrections are certainly not appropriate for the complexes and also are probably not constant among the complexes. Finally, the quadrupole moment of ^{57}Fe is uncertain but is known to be in the range of 0.1–0.3 barn.[3,17]

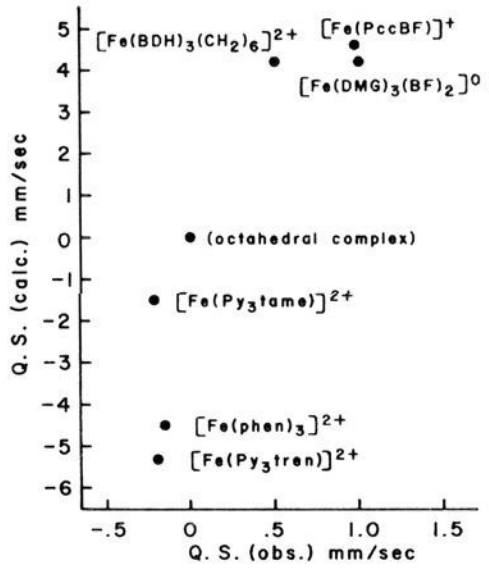

Figure 1. Plot of calculated vs. observed quadrupole splittings for some pseudo-D_3 low-spin ferrous complexes.

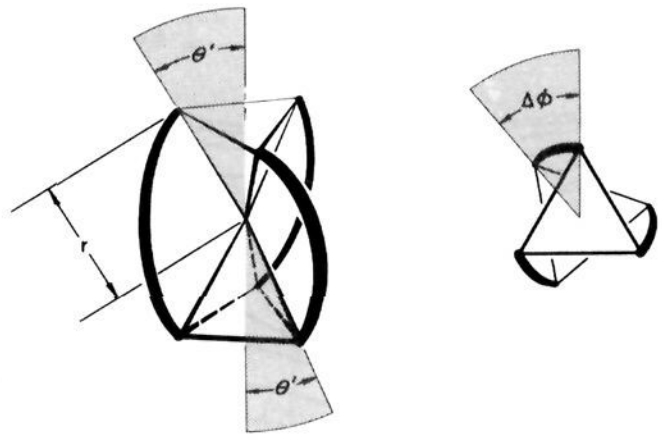

Figure 2. Definition of structural parameters, r, θ', and $\Delta\phi$ used in describing coordination polyhedra of pseudo-D_3 complexes.

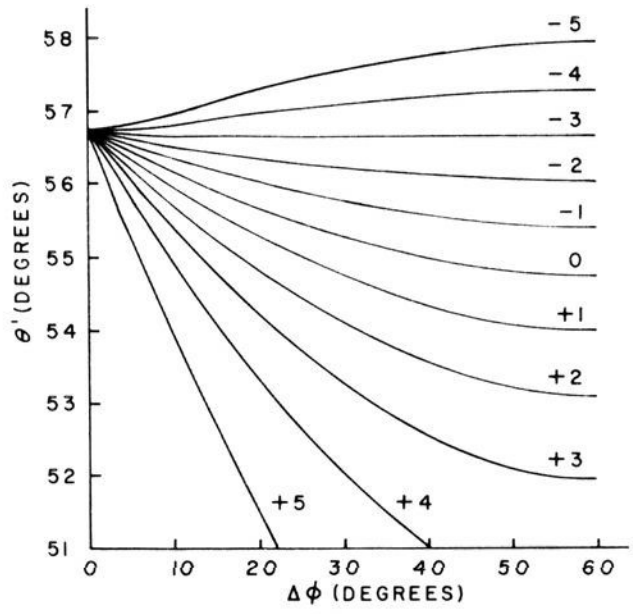

Figure 3. Constant quadrupole splitting contours on the θ' vs. $\Delta\phi$ quadrupole splitting surface (r = constant = 1.93 Å).

The second and third "problems" above cannot be remedied without much further theoretical work; however, the first problem can be investigated using the model presented herein. In an effort to estimate the effect of the magnitude of the point charges and distances at which these charges are placed, several calculations were performed. Variation of the point charges for $[Fe(DMG)_3(BF)_2]$ in the range -0.05 to -0.5, all at the observed crystallographic positions produced a range of qs values from +4.45 to +4.34, a change of about 2%. Over the same range of charge, η varies between 0.0013 and 0.0045. For $[Fe(PccBF)]^+$ and $[Fe(phen)_3]^{2+}$ much more extreme charge and distance values were employed. Charges of -2.0 were placed at the observed crystallographic positions except that the distance to the metal ion was reduced by 0.5 Å from the observed. These values were selected as limiting parameters in that an extreme picture of the bonding in these complexes places the two lone pair electrons on the six nitrogen atoms roughly at the observed bonding distance minus the expectation value of r for 2s or 2p orbitals on the nitrogen atoms. The values calculated for the qs are +2.7 and -1.8 mm/s for $[Fe(PccBF)]^+$ and $[Fe(phen)_3]^{2+}$, respectively. These values still possess the correct sign. Thus, in spite of all the approximations, the model correctly predicts the sign of the qs in these six cases. To our knowledge, no other model has been used to correctly predict the sign of the qs for all the complexes in Table III.[20]

Since a set of six point charges (each of value -0.2e) was used to do each of the calculations leading to the results found in Table III, it is obviously the spatial arrangement of the charges which accounts for the different values of the calculated qs for the various sets. The spatial arrangement for any particular set of point charges (ligating atoms) is conveniently described in terms of the parameters θ' and $\Delta\phi$ (Figure 2) and r where r is the distance from the origin (metal ion) to the point charge (ligating atom). It is to be noted that the mean values of θ' and $\Delta\phi$ for the complexes listed in Table III range from 50.8° to 59.0° and 20.8° to 54.0°, respectively (Table IV). In an effort to find the dependency of the calculated qs on the two structural parameters θ' and $\Delta\phi$, calculations were performed with sets of six point charges describing 195 different spatial arrangements with D_3 symmetry. The point charges were held constant at -0.2e, and r was held constant at 1.93 Å. The results of the calculations are shown in Figure 3. Each solid line represents a constant value for the calculated qs. Considered together, these lines describe a contoured surface (of calculated qs) which varies as a function of both θ' and $\Delta\phi$.

As must be the case the calculated value of qs is zero when $\Delta\phi = 60.0°$ and $\theta' \sim 54.7352°$, the two values characteristic of an octahedron. However, the presence of a zero qs contour line shows that the influence of θ' and $\Delta\phi$ can exactly cancel each other for certain nonoctahedral coordination polyhedra as well. The following general feature of the diagram also merits mention. Regardless of the value of $\Delta\phi$ a negative qs results when θ' is larger than ~56.5° and a positive qs results when θ' is smaller than ~54.7352°.

At $\Delta\phi$ values near zero the surface is very steep and there is a discontinuity in the qs near $\theta' = 56.7°$ where the qs "jumps" from large positive to large negative values. An explanation for this discontinuity can be seen from a superposition of crystal field energy diagrams for some of the cases spanning ranges of θ' from 51° to 58° and $\Delta\phi$ from 0° to 60° (shown in Figure 4). In the figure each line designates how the energy of an orbital of given symmetry and $\Delta\phi$ varies with θ'. It should be noted that at $\Delta\phi = 0°$ the symmetry of the coordination polyhedron is D_{3h} for all θ', whereas at all other $\Delta\phi$ and θ' the symmetry is D_3. Thus, in the D_{3h} case the d orbitals (split into a_{1g}, e', and e'' orbitals) cannot mix and a crossover takes place at $\theta' \approx 56.7°$. At this crossover the d orbital configuration changes from $a_{1g}^2e'^4$ to $a_{1g}^2e''^4$. The change in d orbital configuration causes a large discontinuous change in the qs because the $a_{1g}^2e'^4$ configuration has electron density in the d_{xy} and $d_{x^2-y^2}$ orbitals which contribute positively to the efg and the $a_{1g}^2e''^4$ configuration has electron density in the d_{xz} and d_{yz} orbitals which contribute negatively to the efg (see eq 4 and 5 and Table II). In real complexes, the sharp discontinuity would not occur because as θ' becomes close to the crossover value, the $d_{x^2-y^2}$, d_{xy}, and d_{yz} orbitals are nearly degenerate. Therefore, spin states other than the low-spin one would be expected to become the ground state, and different magnetic as well as Mössbauer parameters would be expected. In order to interpret the qs values for complexes with $\Delta\phi$ near zero, a more sophisticated model including contributions from several spin states is needed. When $\Delta\phi$ is larger than 0°, the d orbital

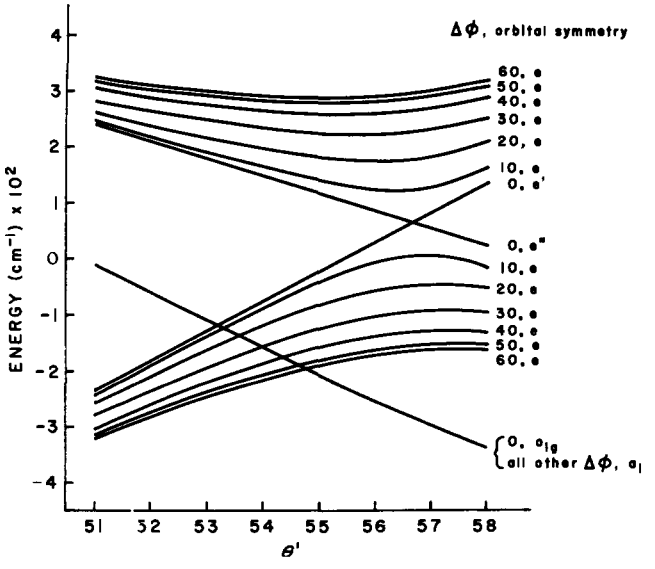

Figure 4. Superposition of crystal field energy diagrams for D_3 or D_{3h} coordination polyhedra as a function of structural parameters θ' and $\Delta\phi$.

configuration does not change throughout the entire range of θ'. Therefore, the discontinuity is avoided for larger $\Delta\phi$ values and the diagram shown in Figure 3 is thus more meaningful for larger $\Delta\phi$ values than it is for $\Delta\phi$ values close to 0.

From the contour diagram, it can be concluded that for a given $\Delta\phi$, the qs changes sign as θ' is varied, whereas for a given θ' the qs changes sign as $\Delta\phi$ is varied only if θ' is in the range 55–56°. Therefore, θ' is the primary structural parameter involved in determining the sign of the qs in complexes described by the D_3 model. Referring back to the structural parameters for the complexes in Table IV and to the contour diagram, we can look at the real complexes in terms of generalized polyhedra. For example, $[Fe(phen)_3]^{2+}$ with $\Delta\phi = 55°$ and $\theta' = 57.7°$ lies in the region of negative qs corresponding to a compressed, near-trigonal antiprism, and $[Fe(DMG)_3(BF)_2]$ with $\Delta\phi = 21°$ and $\theta' = 52.7°$ lies in the positive qs region corresponding to an elongated polyhedron twisted between a trigonal prism and a trigonal antiprism.

C. Complexes with D_{2h} or Pseudo-D_{2h} Symmetry. The final arrangement of point charges to be discussed features a rectangular array of four charges, Z, and two other charges, Z', located on a line perpendicular to the rectangle and passing through its center. This arrangement possesses D_{2h} symmetry and can serve as a reasonable representation for complexes containing two monodentate ligands in the Z' or trans positions and four nitrogen atoms from either two α-dioxime[31] or two α-diimine[32] moieties in the Z or rectangular positions.

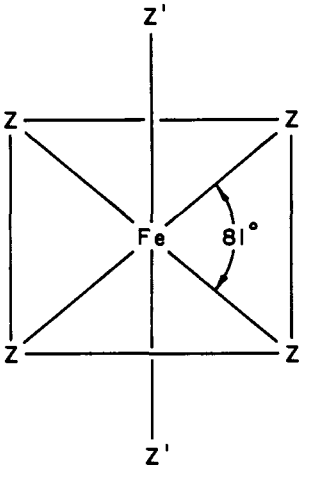

Table V. Parameters Selected for the D_{2h} Systems

Case	M-Z	M-Z'	Z	Range of the ratio: Z'/Z
A	1.93 Å	1.93 Å	−0.2	0 → 1.5
B	1.43 Å	1.43 Å	−1.0	0 → 1.5
C	1.43 Å	1.43 Å	−2.0	0 → 1.0

Table VI. Diagonal Efg Tensor Elements[a]

	Z'/Z = 0.6	Z'/Z = 1.0
Case A	−3.86 (−3.81)	−6.82 (−6.82)
	−35.75 (−35.21)	−12.02 (−11.70)
	39.60 (39.02)	18.84 (18.52)
Case B	−11.88 (−11.31)	−3.79 (−3.79)
	−21.61 (−15.04)	−9.98 (−6.12)
	33.49 (26.35)	13.76 (9.91)
Case C	−11.88 (−10.74)	−3.79 (−3.79)
	−21.61 (−8.48)	−9.98 (−2.27)
	33.49 (19.22)	13.76 (6.06)

[a] The first number is the orbital contribution only, the number in parentheses is the orbital plus point charge value.

The specific geometry to be discussed here is based on the single-crystal x-ray diffraction study[32] of $[Fe(TIM)(CH_3CN)_2](PF_6)_2$[33] where TIM[34] is a 14-membered macrocyclic ligand containing two α-diimine units. As in the case of the pseudo-D_3 complexes the application of the model for calculating the qs requires the selection of values for the metal-charge distances and for the charges. However, the selection of values for the charges is significantly less straightforward than for the six specific pseudo-D_3 complexes considered previously in this paper (see Tables III and IV) where a charge (e.g., −0.2e) was used to represent each of the ligating atoms. In the case of the D_{2h} or pseudo-D_{2h} systems, it seems clearly inappropriate to set all the charges equal to each other (i.e., $Z = Z'$) except in those applications meant to represent complexes where the ligand field strengths of the planar and axial ligands are very similar. It is to be strongly noted that in many complexes containing either two α-dioxime or two α-diimine moieties in the rectangular positions, the axial ligands are clearly weaker (in the spectrochemical sense) than the planar ones.[33,35-38] When performing calculations with $Z \neq Z'$, it is convenient to report the results in terms of the ratio, Z/Z'.[38] Of course, it is also necessary to specify the absolute charge of either Z or Z' and to specify both the M-Z and M-Z' distances.

Various values for the M-Z or M-Z' distances (based on the observed structure of $[Fe(TIM)(CH_3CN)_2]^{2+}$ in the PF_6^- salt[32]), the magnitude of the charge, Z, and the ratio, Z'/Z, were selected for performing the calculations (see Table V and Figures 5 and 6). In case A (Table V) the M-Z and M-Z' distances are the ones found for Fe-N in the single-crystal x-ray diffraction study of $[Fe(TIM)(CH_3CN)_2](PF_6)_2$[32] and Z is given a charge reasonably typical of those computed for ligating atoms in molecular orbital calculations. Cases B and C, with the shorter distances and higher charges represent limiting situations comparable to those discussed previously for the D_3 or pseudo-D_3 complexes. The results of the computations for the three cases are shown in Figures 5 and 6 where η, qs, one-electron d orbital energies and V_{zz}, V_{yy}, and V_{xx} are displayed as a function of Z'/Z.

In all the results the orbital influence is the dominant one in determining the sign of the qs in the range of physically meaningful charge magnitudes and Z'/Z ratios (Table VI). As can be seen in Table VI, these orbital contributions (i.e.,

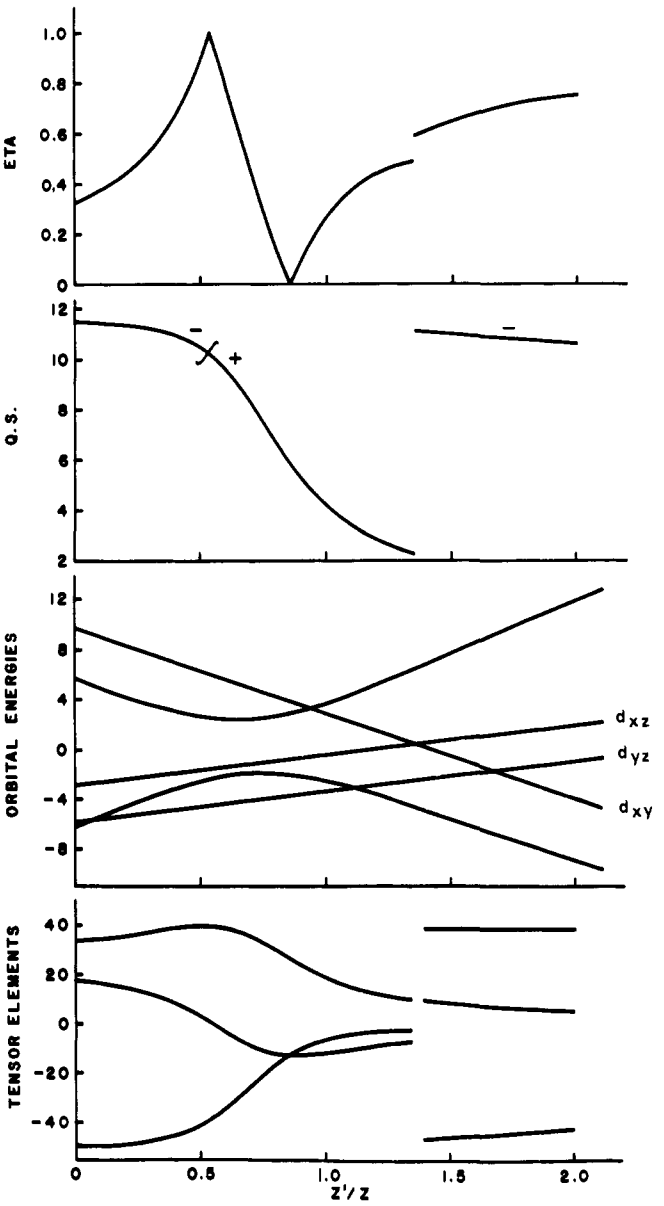

Figure 5. Computational results of η, qs, crystal field orbital energies and the diagonal efg tensor elements for D_{2h} $FeZ_4Z'_2$ models: one Z-Fe-Z = 81°; Z = −0.2e; Fe-Z = Fe-Z' = 1.93 Å; the horizontal axis is common to all portions of the figure; qs in mm/s; η and efg tensor elements defined conventionally (see text); orbital energies $\times 10^{-2}$ cm^{-1}; orbital energy labels refer to coordinate system where X axis bisects 81° angle and Z axis is collinear with Z'-Fe-Z' line (case A, see text).

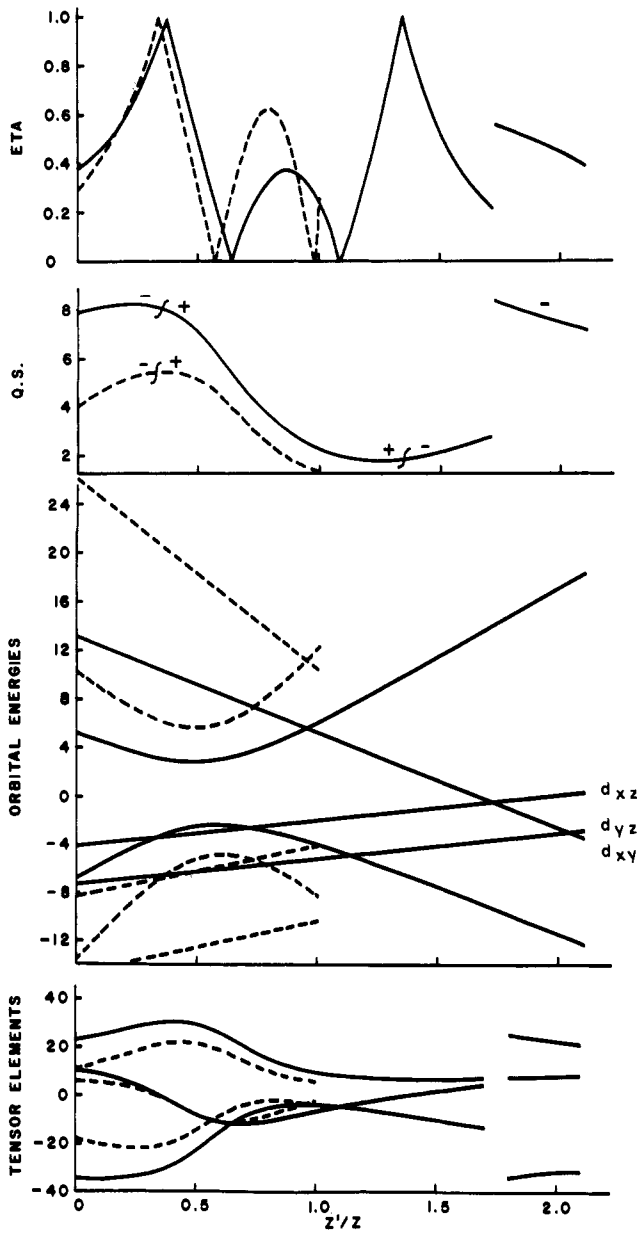

Figure 6. Computational results of η, qs, crystal field orbital energies and the diagonal efg tensor elements for D_{2h} $FeZ_4Z'_2$ models: same notation as in Figure 5 except orbital energies $\times 10^{-3}$ cm^{-1} and Fe-Z = Fe-Z' = 1.43 Å; solid lines, Z = −1.0e; dotted lines, Z = −2.0e (cases B and C, see text).

the diagonal efg tensor elements arising from the six 3d electrons in the crystal field orbitals) are dependent on the M-Z,Z' distances and on Z'/Z but independent of Z for fixed M-Z,Z' distances and for fixed Z'/Z.

Inspection of Figures 5 and 6 reveals that the detailed application of the model to an actual complex requires that "proper" distances and charges be assigned to the two kinds of ligating atoms, trans and planar, in the complex. Given the difficulties of justifying any such detailed assignments it is appropriate to look at the gross qualitative features of the results in terms of available experimental data rather than at the quantitative features.

For all three cases the predicted sign of the qs is positive in the Z'/Z ratio range of 0.54-1.0. Further, in all cases the magnitude of the qs diminishes monotonically as Z'/Z changes from 0.54 to 1.0. In terms of actual complexes most of this range of Z'/Z values (except for Z'/Z = 1) corresponds to species in which the trans or axial ligands occupy a lower place on the spectrochemical series than do the planar ligands. As stated previously, this is the condition that obtains with many complexes studied to date.[33,35,36] For such complexes there are two reasons to believe that the model advanced here is reasonable: (1) For three derivatives of $[Fe([14]\text{-}1,3,8,10\text{-}tetraeneN_4)X_2]^{n+}$ the qs is assigned a positive value.[36] In the three derivatives, where X = NCS^-, or CH_3CN or NO_2^-, the trans ligands are lower[39] on the spectrochemical series than the planar ligand ([14]-1,3,8,10-tetraeneN$_4$), the geometry of which should be *very similar* to TIM.[32,33] (2) In the series of complexes $[Fe([14]\text{-}1,3,8,10\text{-}tetraeneN_4)X_2]^{n+}$, as the ligand field strength of X increases the qs decreases in magnitude, an observation in keeping with the prediction made by the model. Further, in the pairs of complexes $[Fe(niox)_2(imidazole)_2]$ and $[Fe(niox)_2(imidazole)(CO)]$,[35] $[Fe(niox)_2(imidazole)_2]$ and $[Fe(niox)_2(imidazole)(CN)]$,[35] $[Fe(TIM)(NH_3)_2]^{2+}$ and $[Fe(TIM)(NH_3)(CO)]^{2+}$,[41] $[Fe(TIM)(CH_3CN)_2]^{2+}$ and $[Fe(TIM)(CH_3CN)(CO)]^{2+}$,[33]

and $[Fe(TIM)(CH_3NH_2)_2]^{2+}$ and $[Fe(TIM)(CH_3NH_2)(CO)]^{2+}$,[41] the carbon monoxide or cyanide derivative always has the smaller qs. Since the substitution of CO or CN^- for one of the trans donors would be expected to significantly enhance the net field strength of the trans ligands, the reduced magnitude of the qs which is observed for the CN^- or CO derivative is certainly in keeping with the model.

Acknowledgment. This work was supported in part by National Science Foundation Grants GP-23209 and GP-43501X.

References and Notes

(1) (a) G. M. Bancróft and R. H. Platt, *Adv. Inorg. Nucl. Chem.*, **15**, 59 (1972); (b) G. M. Bancroft, *Coord. Chem. Rev.*, **11**, 247 (1973).
(2) H. Eicher and A. Trautwein, *J. Chem. Phys.*, **50**, 2540 (1969).
(3) R. Ingalls, *Phys. Rev. A*, **133**, 787 (1964).
(4) G. M. Bancroft, M. J. Mays, and B. E. Pratter, *J. Chem. Soc. A*, 956 (1970).
(5) M. G. Clark, A. G. Maddock, and R. H. Platt, *J. Chem. Soc., Dalton Trans.*, 281 (1972).
(6) C. D. Pribula, T. L. Brown, and E. Münck, *J. Am. Chem. Soc.*, **96**, 4149 (1974).
(7) (a) R. M. Sternheimer, *Phys. Rev.*, **130**, 1423 (1963); (b) for a discussion of Sternheimer effects, see E. A. C. Lucken, "Nuclear Quadrupole Coupling Constants", Academic Press, New York, N.Y., 1969.
(8) W. A. Goddard III, and B. A. Olafson, *Proc. Natl. Acad. Sci. U.S.A.*, **72**, 2335 (1975).
(9) R. V. Parish, *Prog. Inorg. Chem.*, **15**, 101 (1972).
(10) R. L. Collins and J. C. Travis in "Mössbauer Effect Methodology", Vol 3, Plenum Press, New York, N.Y., 1967, pp 123–161.
(11) H. Eicher and A. Trautwein, *J. Chem. Phys.*, **50**, 2540 (1969).
(12) T. L. Brown, *Acc. Chem. Res.*, **7**, 408 (1974).
(13) A. J. Freeman and R. E. Watson, *Phys. Rev.*, **131**, 2566 (1963).
(14) R. Ingalls, *Phys. Rev.*, **128**, 1155 (1962).
(15) E. Clementi, *I.B.M. Corp. Syst., J.*, Table 37-01 (1965).
(16) C. F. Jackels, private communication.
(17) A. J. Nozik and M. Laplan, *Phys. Rev.*, **159**, 273 (1967).
(18) M. Pasternak, A. Simopoulous, and Y. Hazony, *Phys. Rev. A*, **140**, 1892 (1965).
(19) R. V. Parish and R. H. Platt, *Inorg. Chim. Acta*, **4**, 65 (1970).
(20) W. M. Reiff, *J. Am. Chem. Soc.*, **95**, 3048 (1973); private communication, to be submitted for publication.
(21) This value for the net charge or ligating sp^2 nitrogen atoms seems reasonable based on EXTENDED Hückel MO calculations on similar systems; unpublished results by S. C. Jackels and E. R. Davidson.
(22) Arguments have been advanced (M. A. Robinson, J. D. Curry, and D. H. Busch, *Inorg. Chem.*, **2**, 1178 (1963); P. Krumholtz, *Struct. Bonding (Berlin)*, **9**, 139 (1971)) which relate the lowest energy spin allowed transition in tris-α-diimine nickel(II) complexes to the ligand field strength of these ligands with respect to the analogous Fe(II) complex. In this context both py_3tame and py_3tren are similar to the symmetrical ligands bpy and pyridinalmethylimino (see L. J. Wilson and N. J. Rose, *J. Am. Chem. Soc.*, **90**, 6041 (1968), and E. Larsen, G. N. LaMar, B. E. Wagner, J. E. Parks, and R. H. Holm, *Inorg. Chem.*, **11**, 2652 (1972)). Thus, representing all the ligating atoms by a charge in these two cases seems justified. For, the PccBF ligand the arguments which justify the use of a single charge rather than two different charges are not as strong in view of the relatively low transition energy for the first spin allowed transition of $[Ni(PccBF)]^+$ (see Larsen et al.).
(23) The authors are grateful for the discussion of the referee concerning this point, also see ref 12.
(24) M. Dunaj-Jurco and E. C. Lingafelter, private communication.
(25) M. R. Churchill and A. H. Reis, Jr., *Inorg. Chem.*, **11**, 2299 (1972).
(26) V. L. Goedken, J. Pluth and S. Peng, Abstracts of the American Crystallographic Association Meeting, Summer, 1973, No. P2, p 189.
(27) A. Zalkin, D. H. Templeton, and T. Ukei, *Inorg. Chem.*, **12**, 1641 (1973).
(28) E. C. Lingafelter, private communication.
(29) C. Mealli and E. C. Lingafelter, *Chem. Commun.*, 885 (1970).
(30) E. B. Fleischer, A. E. Gebala, D. R. Swift, and P. A. Tasker, *Inorg. Chem.*, **11**, 2775 (1972).
(31) (a) C. K. Prout and T. J. Wiseman, *J. Chem. Soc.*, 497 (1964); (b) K. Bowman, A. P. Gaughan, and Z. Dori, *J. Am. Chem. Soc.*, **94**, 727 (1972).
(32) H. W. Smith and E. C. Lingafelter, private communication.
(33) D. A. Baldwin, R. M. Pfeiffer, D. W. Reichgott, and N. J. Rose, *J. Am. Chem. Soc.*, **95**, 5152 (1973).
(34) The TIM ligand provides its four nitrogen atoms in a plane containing the metal ion but some of the carbon atoms in this macrocyclic ligand are not in that plane. Thus, the ligating atoms in $[Fe(TIM)X_2]^{n+}$ complexes can possess D_{2h} symmetry but the entire complex cannot.
(35) B. W. Dale, R. J. P. Williams, P. R. Edwards, and C. E. Johnson, *Trans. Faraday Soc.*, **64**, 620, 3011 (1968).
(36) J. C. Dabrowiak, P. H. Merrell, J. A. Stone, and D. H. Busch, *J. Am. Chem. Soc.*, **95**, 6613 (1973).
(37) C. K. Jorgensen, "Modern Aspects of Ligand Field Theory", North-Holland Publishing Company, Amsterdam, 1971 Chapter 26.
(38) R. A. LaRossa and T. L. Brown, *J. Am. Chem. Soc.*, **96**, 2072 (1974).
(39) See ref 36 and 40 for a discussion concerning the placement in the spectrochemical series of planar macrocyclic ligands containing two α-diimine linkages.
(40) S. C. Jackels, K. Farmery, E. K. Barefield, N. J. Rose, and D. H. Busch, *Inorg. Chem.*, **11**, 2893 (1972).
(41) D. W. Reichgott and N. J. Rose, unpublished results.

Oxidative Addition of Benzyl Halides to Zero-Valent Palladium Complexes. Inversion of Configuration at Carbon

K. S. Y. Lau, P. K. Wong, and J. K. Stille*

Contribution from the Department of Chemistry, University of Iowa, Iowa City, Iowa 52242. *Received February 23, 1976*

Abstract: Inversion of configuration at carbon (90–100%) was observed during the oxidative addition of optically active α-phenethyl bromide and benzyl-α-*d* chloride to either tetrakis(triphenylphosphine)palladium(0) (**1**) in the presence of carbon monoxide or carbonyltris(triphenylphosphine)palladium(0) (**4**). The product acylpalladium(II) complex in each case was formed in high yield and was converted to the corresponding optically active ester. In the absence of carbon monoxide, benzyl-α-*d* chloride underwent oxidative addition to **1** to give a stable alkylpalladium(II) complex which was transformed into the acylpalladium complex via carbon monoxide insertion. The acylpalladium complex obtained in this manner yielded the corresponding optically active ester which did not contain as high a degree of optical purity (~75% net inversion). The cause of racemization was attributed to a nucleophilic exchange equilibrium process during the oxidative addition of benzyl-α-*d* chloride to **1**.

Three different types of mechanisms have been proposed for the oxidative addition of alkyl halides to low valent group 8 transition metal complexes: (a) nucleophilic displacement of halogen by attack of the metal at the carbon center,[1–8] (b) metal insertion into the carbon–halogen bond via a three-centered transition state,[9–12] and (c) homolytic carbon–halogen cleavage involving the intermediacy of carbon radicals.[13–20]

The isolation of racemized products and the retarding effect on the rate of reaction by radical scavengers have been offered as evidence for the involvement of radical intermediates in the oxidative addition of alkyl halides to d^8 iridium(I),[14] d^{10}